ELSEVIER

Journal of Power Sources 97–98 (2001) 423–426

JOURNAL OF POWER SOURCES

www.elsevier.com/locate/jpowsour

Synthesis and structures of lithium manganese oxide spinel, $LiMn_2O_{4-\delta}$ ($0 \leq \delta \leq 0.27$)

Ryoji Kanno[a,*], Masao Yonemura[a], Tomoko Kohigashi[a], Yoji Kawamoto[a], Mitsuharu Tabuchi[b], Takashi Kamiyama[c]

[a]*Faculty of Science, Department of Chemistry, Kobe University, 1-1 Rokko-dai, Nada, Kobe 657-8501, Japan*
[b]*Osaka National Research Institute, 1-8-1 Midorigaoka, Ikeda 653-8577, Japan*
[c]*Institute of Materials Structure Science, High Energy Accelerator Research Organization, Tsukuba 305-0801, Japan*

Received 27 June 2000; received in revised form 11 January 2001; accepted 13 January 2001

Abstract

Lithium manganese oxides spinels were synthesized under various synthesis conditions and their structures were determined by TOF neutron powder diffraction measurements. Oxygen vacancies exist for the samples synthesized above 800°C, and the amount of vacancies was found to be sensitive to the synthesis conditions. The nearly stoichiometric spinels were synthesized at 750°C in O_2 followed by heating at 470°C. The transition temperatures of the cubic–orthorhombic transitions and the magnetic properties varied with the compositions. The stoichiometric spinel showed no cubic–orthorhombic phase transition. © 2001 Elsevier Science B.V. All rights reserved.

Keywords: Lithium manganese spinel; Phase transition; Neutron structure analysis

1. Introduction

Lithium manganese oxide spinels are usually discussed in terms of the triangular composition region $LiMn_2O_4$–$Li_4Mn_5O_{12}$–$Li_2Mn_4O_9$. Changes in the Li:Mn ratio for $Li_{1+x}Mn_{2-x}O_4$ leads to compositions along the tie line from $LiMn_2O_4$ to $Li_4Mn_5O_{12}$, and decreasing the heating temperature from 900°C varies the composition from $LiMn_2O_4$ towards $Li_2Mn_4O_9$. The structures and the relationships of the $LiMn_2O_4$–$Li_4Mn_5O_{12}$–$Li_2Mn_4O_9$ phase diagram are still ambiguous. Furthermore, the structure is complicated due to the existence of Jahn–Teller trivalent manganese ions; the Jahn–Teller phase transition is accompanied by a symmetry reduction from cubic [1,2], and the transitions seemed to be dependent on the sample synthesis conditions [3].

The thermogravimetry study of the spinel indicated weight loss at high temperatures [4], and the structure model of the oxygen vacancy phase was considered based on thermal measurements [5]. However, the nature of the oxygen vacancy in the spinel structure is still unclear. For example, two structural models have been proposed for the spinel with the nominal composition, $LiMn_2O_{4-\delta}$; the oxygen deficient spinel $LiMn_2O_{4-\delta}$ with the vacancy clustering [5], and the excess cation model with interstitial cations at the 16*c* octahedral sites in Fd^3m space group [6]. We previously reported the structure of the cubic manganese spinel synthesized at 900°C using neutron diffraction [7] and indicated the oxygen vacancy at 32*e* site with interstitial oxygen at 8*b* site. The results also indicated that the amount of the vacancy is dependent on the synthesis conditions.

In the present study, the relationship between the structure and the synthesis conditions of the lithium manganese spinels were clarified for samples synthesized using various conditions. The structures have been determined by neutron powder diffraction measurements. Low-temperature phase transitions were also studied for the samples characterized by the diffraction methods using powder X-ray diffraction (XRD) and differential scanning calorimetry (DSC) measurements.

2. Experimental

The lithium manganese spinels were prepared by heating appropriate molar ratios of Li_2CO_3 and Mn_2O_3. They were mixed, pressed into pellets, and heated at 750–1000°C in an oxygen atmosphere. The spinels close to the stoichiometric compositions were synthesized from the starting materials of manganese oxides obtained by thermal decomposition of manganese oxalate. The appropriate molar ratios

* Corresponding author. Tel.: +81-78-803-5681; fax: +81-78-803-5681.
E-mail address: kanno@kobe-u.ac.jp (R. Kanno).

PII: S0378-7753(01)00687-5

Table 1
Neutron diffraction results on the spinels synthesized at various conditions

Composition	Starting materials	Occupation parameters at the oxygen 32*e* site *g*(O)	Lattice parameter, *a* (Å)	Synthesis temperature, *T* (°C)	Atmosphere	Li:Mn ratio	Cooling rate (°C/min)	Impurity
$LiMn_2O_{4-\delta}$, $\delta = 0.132$ (sample A)	Li_2CO_3, Mn_2O_3	0.967(3)	8.24609(17) at 325 K	900	O_2	0.5	100	None
$LiMn_2O_{4-\delta}$, $\delta = 0.088$ (sample B)	$LiOH{\cdot}H_2O$, MnO_x	0.9707(11)	8.24203(14) at 325 K	470 (three times)	Air/Air	0.5	60	None
$LiMn_2O_{4-\delta}$ $\delta \approx 0.0$ (sample C)	$LiOH{\cdot}H_2O$, MnO_x	0.0	8.23634(13) at 300 K	470 (three times)	Air/O_2	0.5	60	None

of $LiOH{\cdot}H_2O$ and manganese oxide were mixed and heated at 750–800°C in air or in oxygen atmosphere after preheating at 470°C from one to three times. In order to confirm the existence of oxygen vacancy in the structure, the structures of the samples treated with titanium metal and with introduced oxygen vacancies were determined by neutron diffraction measurements.

XRD patterns of the powdered samples were collected using an X-ray diffractometer (Rigaku RAD-C, 12 kW) with Cu Kα radiation. The diffraction data were collected with a 0.02° step-width over a 2θ range from 20 to 110°. Low-temperature XRD patterns were obtained in the temperature range 10–300 K.

Neutron diffraction data for the spinels was obtained between 5 and 325 K on time-of-flight (TOF) neutron powder diffractometers, VEGA and Sirius, at the KENS pulsed neutron spallation source at the High Energy Accelerator Research Organization (KEK). The structural parameters were refined with RIETAN98T [8]. DSC was measured by a TAS-200 (Rigaku) between 150 and 360 K at heating and cooling rates of 10 K/min.

3. Results and discussion

3.1. Synthesis and structures of the spinels

The manganese spinels were divided into four categories: oxygen deficient, lithium-substituted, cation deficient, and near-stoichiometric $LiMn_2O_4$. Table 1 summarizes the neutron diffraction results of typical samples synthesized in the present study. Oxygen deficient spinels were synthesized at 900°C using Mn_2O_3 and Li_2CO_3 as starting materials. The ionic distribution of the spinels with a Li:Mn ratio of 0.5 were determined at 325 K to be $[Li_1]_{tetra}(Mn_2)_{octa}O_{4-\delta}$ ($\delta = 0.132$, $g(O) = 0.967(3)$) with a small fraction of oxygen vacancies at the 32*e* site (sample A).

3.2. Oxygen vacancy introduced by titanium metal treatment

The spinels synthesized at 900°C in O_2 were used for the treatments. Both the spinel and titanium metal powder were placed separately in small Au crucibles, which were placed in a quartz tube and sealed under vacuum. The structure of the samples treated at 600°C for 12 h was determined by the neutron diffraction; the data was collected both for the samples containing ^7Li and "natural abundance" lithium. No interstitial cations or anions were found in the structure, and the oxygen vacancy fraction increased from 0.132(12) to 0.276(16).

3.3. The stoichiometric spinels

Starting materials with higher reactivity were used to synthesize the stoichiometric spinels in the present study. The spinels close to the stoichiometric composition were obtained from the starting materials, $LiOH{\cdot}H_2O$ and MnO_x, which was obtained by the thermal decomposition of manganese oxalate. One sample was heated at 470°C several times before being reacted at 750°C in O_2 (sample C). Several structure models were considered during the refinements; vacancies at the 8*a* lithium site, 16*d* manganese site, and 32*e* oxygen site, cations in the interstitial 16*c* site, and disordering at the manganese and lithium sites. However, no significant deviation from stoichiometric composition was observed at the lithium 8*a* and manganese 16*d* sites, and no cations were found at the interstitial 16*c* sites. On the other hand, the sample synthesized with a final heat treatment at 750°C in air (sample B) showed a small fraction of oxygen vacancies (about 2%).

Three typical examples of the spinel-types have been indicated: the spinel with oxygen vacancies synthesized from Li_2CO_3 and Mn_2O_3(about 3.3% vacancies, sample A), the spinel close to the stoichiometric composition (about 2% vacancies, sample B), and the stoichiometric spinel $LiMn_2O_4$ synthesized from $LiOH{\cdot}H_2O$ and MnO_x (sample C). The phase transitions were studied for these spinels using powder XRD and DSC measurements.

3.4. Phase transitions in the spinels

Fig. 1 shows the DSC curves of the oxygen deficient spinel (sample A) ($\delta = 0.132$), sample B ($\delta = 0.088$), and the stoichiometric spinel (sample C) ($\delta \approx 0.0$). The

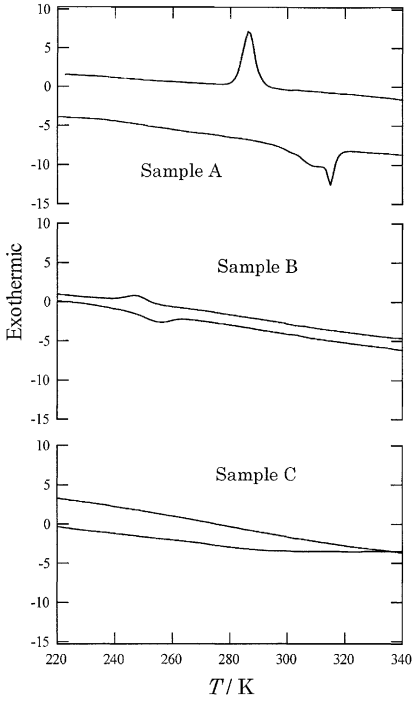

Fig. 1. DSC curves of the oxygen deficient spinel (sample A) ($\delta = 0.132$), sample B ($\delta = 0.088$), and the stoichiometric spinel (sample C) ($\delta \approx 0.0$).

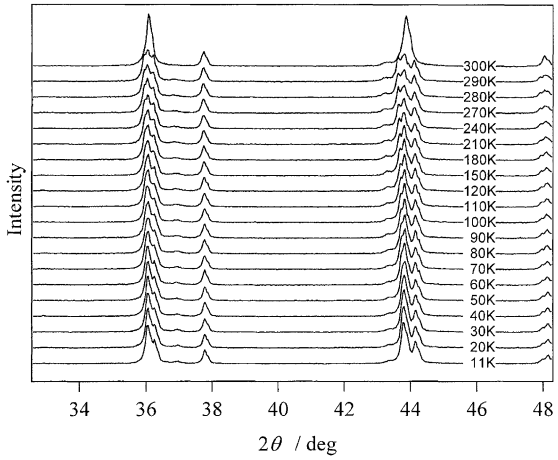

Fig. 2. Low-temperature X-ray diffraction (XRD) patterns for sample A synthesized from Li_2CO_3 and Mn_2O_3 at 900°C in O_2.

transitions were observed around 300 and 250 K for samples A and B, respectively; these results are consistent with those reported by Sugiyama et al. [5]. However, the stoichiometric spinel (sample C) showed no significant anomaly in the DSC curves down to 150 K.

Figs. 2 and 3 show the low-temperature XRD patterns for samples A and C. Low-temperature structures of the oxygen-deficient spinel with $\delta = 0.132$ (sample A) were determined in the $3a \times 3a \times a$ superlattice structure with the orthorhombic space group *Fddd* [9]. The low-temperature structure of sample A was determined using neutron diffraction data, where oxygen vacancies was taken into account for the refinement of our structure model [10].

No significant change was found in the XRD patterns down to 10 K for sample C with $\delta \approx 0.0$. This indicates that the stoichiometric spinel showed no phase transition concerning Jahn–Teller ordering at low-temperatures. This is consistent with the DSC results indicated in the present study.

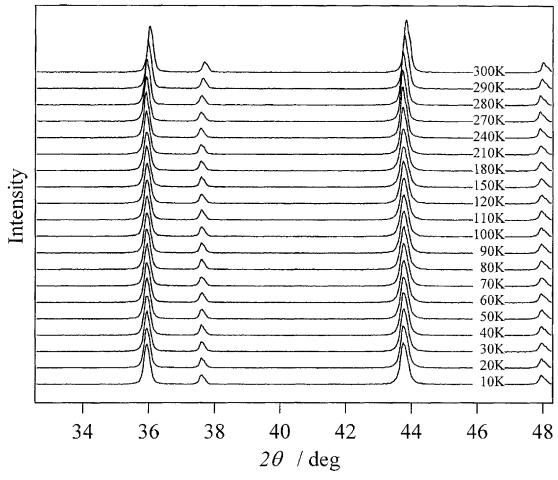

Fig. 3. Low-temperature XRD patterns for sample C synthesized from $LiOH{\cdot}H_2O$ and MnO_x at 470°C in air and 750°C in O_2.

4. Conclusion

The neutron diffraction results indicated that the composition of the lithium manganese spinel is dependent on the synthesis conditions. The reaction at 750–900°C using Li_2CO_3 and Mn_2O_3 leads to oxygen vacancies. The fraction of oxygen vacancies was sensitive to the heating conditions. The existence of oxygen vacancies was confirmed by titanium metal treatment in evacuated sealed tubes. The fraction of oxygen vacancies decreased as the synthesis temperature was varied from 900 to 750°C, and decreased with increasing lithium content in $Li_{1+x}Mn_{2-x}O_4$ synthesized at 900°C [10]. The effect of increasing lithium content in the spinel on the electrochemical properties is well known; the cycling characteristics improve with increasing lithium content. This is partly because of the decrease in the oxygen vacancies with increasing lithium content. The spinels close to the stoichiometric composition, $LiMn_2O_4$, were obtained from the starting materials, MnO_x obtained by the thermal decomposition of manganese oxalate and $LiOH{\cdot}H_2O$ with a reaction heated at 470°C in air and 750°C in O_2. The characteristics of the phase transitions in the spinel were confirmed for the samples characterized in the present study.

Acknowledgements

This work was supported partly by a Grant-in-Aid for Scientific Research from The Ministry of Education, Science and Culture, and partly by a grant from Genesis Research Institute.

References

[1] A. Yamada, M. Tanaka, Mater. Res. Bull. 30 (1995) 715.
[2] A. Yamada, J. Electrochem. Soc. 122 (1996) 160.
[3] C. Masquelier, M. Tabuchi, K. Ado, R. Kanno, Y. Kobayashi, Y. Maki, O. Nakamura, J.B. Goodenough, J. Solid State Chem. 123 (1996) 255.
[4] A. Yamada, K. Miura, K. Hinokuma, M. Tanaka, J. Electrochem. Soc. 142 (1995) 2149.
[5] J. Sugiyama, T. Atsumi, A. Koiwai, T. Sasaki, T. Hioki, S. Noda, N. Kamegashira, J. Phys.: Condens. Matter 9 (1979) 1729.
[6] M. Hosoya, H. Ikuta, T. Uchida, M. Wakihara, J. Electrochem. Soc. 144 (1997) L52.
[7] R. Kanno, A. Kondo, M. Yonemura, R. Gover, Y. Kawamoto, M. Tabuchi, T. Kamiyama, F. Izumi, C. Masquelier, G. Rousse, J. Power Sources 81 (1999) 542.
[8] F. Izumi, in: R.A. Young (Ed.), The Rietveld Method, Oxford University Press, Oxford, 1993 (Chapter 13).
[9] G. Rousse, C. Masquelier, J. Rodriguez-Carvajal, M. Hervieu, Electrochem. Solid State Lett. 2 (1999) 6.
[10] M. Yonemura, R. Kanno, T. Kohigashi, Y. Kawamoto, M. Tabuchi, T. Kamiyama, H. Kawaji, in preparation.